# Temperature-Dependent Recombination of Triplet Biexcitons in Singlet Fission of Hexacene

Yuqin Qian[1#], Zhi-Chao Huang-Fu[1#], Tong Zhang[1], Xia Li[1], Avetik R. Harutyunyan[2], Gugang Chen[2], Hanning Chen[3]*, Yi Rao[1]*

[1]Department of Chemistry and Biochemistry, Utah State University, Logan, UT 84322
[2]Honda Research Institute, USA, Inc., San Jose, CA 95134, USA
[3]Department of Chemistry, American University, DC 20016

## • Abstract

Singlet fission is a spin-conserving process for the multiplication conversion of one singlet exciton into two individual triplet excitons by absorbing one photon. Such a multiplication is believed to circumvent the Shockley-Queisser thermodynamic limit for improving efficiency of solar energy conversion. A mechanistic understanding of generation and yields of triplet excitons from singlet-fission materials is essential for efficient exploitation of solar energy. Here we employ temperature-dependent transient absorption spectroscopy to examine the dynamical nature of singlet fission and triplet excitons in hexacene. The generation and dissociation rates of the intermediate correlated biexciton, $^1$(TT), are independent of temperature from 77 K to the room temperature. On the other hand, the triplet excitons in spatially separated biexcitons, $^1$(T···T), relax via geminate and non-geminate recombination. The former was found to be temperature-dependent, whereas the latter is temperature-independent. Quantitative analyses of the temperate-dependent rates for the two recombination processes yield the energy difference between the $^1$(T·· ·T) and $^1$(TT), which were further confirmed by our density functional theory (DFT) calculations.

Corresponding Authors: Yi Rao: yi.rao@usu.edu and Hanning Chen: hchen@american.edu
#Y.Q and Z.C.H.F. contributed equally to this work.

- **Introduction**

Singlet fission is a spin-conserving process for the multiplication conversion of one singlet exciton into two individual triplet excitons via the absorption of one photon.[1-2] Such a multiplication has the potential to overcome the so-called Shockley-Queisser limit for further utilization of solar energy. Microscopically, this unique phenomenon goes from the formation of an electronically and spin correlated triplet biexciton, $^1$(TT), followed by the dissociation into a spin-correlated but spatially separated triplet biexciton $^1$(T···T). Eventually, spin decoherence gives two spin-uncorrelated $T_1$ excitons. The mechanism for singlet fission is given by[1-7]

$$\mathbf{S_0 + S_1 \longrightarrow {}^1(TT) \leftrightarrows {}^1(T\cdots T) \longrightarrow T_1 + T_1} \qquad \text{Eq. 1}$$

where $S_0$ represents a ground state, $S_1$ is a singlet exciton, $T_1$ is a triplet exciton, $^1$(TT) is the electronically and spin correlated triplet biexciton that has overall singlet spin, and $^1$(T···T) is the spatially separated triplet biexciton with overall singlet spin.

Some previous studies have demonstrated that the separation of the correlated triplet $^1$(TT) is mediated by a thermally activated hopping process.[8-16] Temperature-dependent transient absorption were used to examine the thermal process in tetracene, pentacene, rubrene, etc.[8-15] For example, the dynamics of singlet exciton fission in tetracene are independent of temperature by Friend and coworkers.[9, 17] They also showed that a $^1$(TT) state exists and is thermally dissociated on 10-100 ns timescales to form free triplets in tetracene. However, Bardeen and coworkers as well as Schmidt and coworkers showed that the rate of the prompt photoluminescence from photoexcited tetracene exhibits no appreciable temperature dependence in photoexcited tetracene.[18-19] Such an observation casts doubt on the long-standing thermally-activated model for tetracene. On the other hand, the dynamics of $^1$(T ··· T) in pentacene exhibit temperature dependence.[11] They found that the time constants for triplet pair separation demonstrate two distinct temperature-dependent regimes of triplet transport. These temperature-dependent singlet fission dynamics on tetracene and pentacene reveal and discern kinetic pathways, enabling us to gain insights into singlet fission of polyacenes. On the other hand, temperature-dependent experiments of singlet fission for hexacene remain unexplored.

Triplet excitons in $^1$(T···T) have been demonstrated to recombine in an enhanced manner during singlet fission at high illuminating fluence.[4, 20-28] It was found that the recombination of triplet excitons in acenes decays through both monomolecular radiative and non-radiative relaxations.[21] Recently, Huang and co-workers showed that the triplet exciton recombination is mediated by singlet excitons within a few nanoseconds in tetracene.[24] They concluded that triplet excitons could interact with each other to produce singlet excitons with transient absorption microscopy. It turned out that the triplet-triplet interactions are thermodynamically exothermic in tetracene. In our early work, we examined anisotropic nature of singlet fission in hexacene single crystals.[29] It was found that both geminate and nongeminate recombination contribute to the relaxations of triplet excitons in hexacene single crystals. The geminate recombination rate is independent of the initial excitation density, while the non-geminate recombination arises likely from triplet-triplet bimolecular energy transfer. These guesses could be verified by magnetic methods as demonstrated in the literature.[21] The rates for both recombination processes were shown to be

anisotropic. However, the properties and temperature-dependent characteristics of the two pathways in hexacene were left unexplored.

In this work, we present temperature-dependent transient absorption experiments of polycrystalline hexacene. Hexacene was chosen because its triplet-triplet conversion into an excited singlet is not anticipated to occur.[20-22, 25, 30] Our goal was to reveal the nature of both $^1$(TT) and $^1$(T···T), as well as study the recombination of triplet excitons in hexacene at low temperatures. Compared with the dynamics at different temperatures, and combined with computational results, we found that the spatially separated $^1$(T···T) state relaxed through both thermally activated and thermally inactivated processes.

- **Experimental section**

**Temperature-dependent Transient absorption spectroscopy.** In our earlier experiments, our transient absorption spectrometer reached only sensitivity of $10^{-3}$ in 10 seconds.[30] To avoid triplet-triplet annihilation, we need a sensitivity of $10^{-5}$ in 1 s with a low fluence for temperature-dependent transient absorption experiments. To that end, a home-built transient absorption spectrometer was constructed for our experiments. In short, a single-unit integrated femtosecond laser system (PHAROS, Light Conversion) with a seed oscillator was used in our experiments as seen in Figure 1(A). The pulse duration was about 290 fs with 100 kHz repetition rate and a center wavelength at 1030 nm. The output power of the laser was 10.0 W in the experiments. 80% of the 1030 nm output was introduced to an optical parametric amplifier (ORPHEUS-ONE, Light Conversion) for the output wavelength of 1400 nm, followed by a beta barium borate (BBO, Foctek) crystal to generate a pump pulse of 710 nm. The remaining 20% of the output laser pulse was focused onto an yttrium aluminum garnet (YAG, Newlight Photonics Inc.) crystal plate to produce a white light super-continuum as a probe light. The probe and pump light beams were focused and overlapped on the sample. Two polarizers were placed to selectively measure the parallel or perpendicular polarized signal relative to the excitation beam. The time delay between the pump beam and the probe beam was controlled by a mechanical delay stage (IMS600PP, Newport). The instrumental response time for the transient absorption experiments was found to be 143 ± 10 fs.

A fast-sampling system for a 100 kHz femtosecond laser was adopted by modifying the scheme in the literature.[31-32] A 150 mm spectrometer (Kymera 193i, Andor) was used to disperse the probe spectra. A line camera with two fast analog-to-digital converters (ADC) (Octoplus, Teledyne e2V), followed by a frame grabber (Xtium-CL MX4, Teledyne DALSA) was used to capture the spectra. A home-built divider synchronized with the laser was used to generate two trigger signals, one with a 20 kHz electrical signal for the camera, and the other with a 20 Hz one for the frame grabber. The pump pulse was modulated by an optical chopper (Model 3501, New Focus) at 5 kHz, which was also synchronized by the laser. Thus, the line camera collected two spectra for each pump on and pump off, which were managed by the two ADCs, separately. The layout of the synchronization unit is shown in Figure 1 (B). The data collection and processing for different time delays were taken with a home-edited Labview program. This transient absorption spectrometer enabled us to readily achieve a sensitivity of $10^{-5}$ with an integration of 1 second. As such, we were able to keep a fluence as low as 1.5 μJ/cm$^2$ in an effort to observe some subtle difference caused by the change in temperature. Temperature-dependent transient absorption

experiments were taken under cryogenic conditions. The cryostat (Microstat N, Oxford) was connected with a vacuum pump. Temperature control was achieved by using a cryogenic temperature controller (MercuryiTC, Oxford).

**Sample preparation.** The precursor of hexacene was synthesized by following the protocol reported in the literature.[30, 33-34] Chemical vapor deposition was used to deposit polycrytalline hexacene films on quartz substrate. The substrate was initially cleaned by a piranha solution, then rinsed with doubly-distilled water, dried in $N_2$ flow, and stored under argon atmosphere prior to use. Hexacene thin films were deposited under $1 \times 10^{-6}$ Torr vacuum. Figure 1(C) shows the visible absorption spectrum of a typical hexacene thin film. The characteristic peak at 860 nm was observed, which is in agreement with those reported in the literature.[30, 34] The thickness of the film was kept at ca. 400 nm with the optical density of 0.8 for transient absorptions.[34]

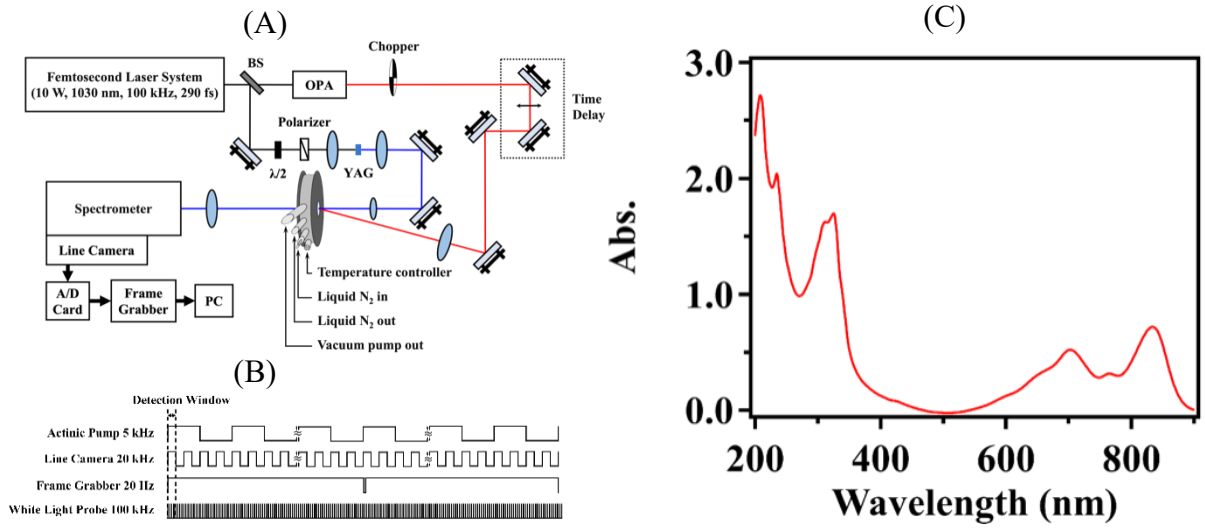


**Figure 1**. (A) Experimental setup for transient absorption measurements. (B) Layout of the synchronization unit. (C) UV-vis absorption of polycrystalline hexacene thin films.

- **Computational Details**

In our molecular simulation, the hexacene thin film was represented as a $9 \times 9 \times 3$ hexacene supercell, whose unit cell lattice vectors of {$a$=7.697Å, $b$=6.306Å, $c$=16.480Å, $\alpha$=91.25°, $\beta$=98.77°, $\gamma$=95.81°} were characterized by X-ray diffraction analysis.[33] Aiming to achieve a compromised balance between accuracy and efficiency, the hybrid quantum mechanics/molecular mechanics (QM/MM) approach[35] was adopted. Specifically, a hexacene molecule and one of its nearest neighbors were chosen as our single fission reaction center that is accurately modeled by the density functional theory (DFT),[36] while all other molecules are efficiently described by the general Amber force field (GAFF).[37] Unless otherwise specified, all simulations were carried out by the open-source CP2K package[38] with the Goedecker-Tetter-Hutter (GTH) pseudopotential,[39] polarized-valence-double-ζ (PVDZ) basis set,[40] long-range-corrected and range-separated

Perdew-Ernzerhof-Burke (LC-ωPBE) functional,[41] electrostatic QM/MM coupling scheme,[42] and wavelet-based Poisson solver.[43]

- **Results**

Figure 2(A) shows two-dimensional pseudo-color plots of transient spectra of hexacene in terms of ΔT/T at two temperatures of 77 and 220 K (those for 100, 150, and 180 K found in Figure S1). The positive changes in ΔT/T centered in the region of 830 - 870 nm and 700-730 nm were mainly assigned to the ground state bleaching (GSB), possibly mixed with some stimulated emission (SE). These positive responses in the transient spectra correspond to those of the linear absorption spectrum in hexacene in Fig. 1 (C), as expected. However, the anticipated positive regions from 730 nm to 830 nm were found to be negative in comparison with the linear optical absorption in Figure 1 (C). On the other hand, six bands show negative signatures, including 515, 575, 600, 730, 790, and 890 nm. In our previous work, the negative spectra from 500 nm to 570 nm were attributed to a mixture of both the singlet excited state absorption ($S_1$-$S_n$) and triplet excited state absorption ($T_1$-$T_n$).[29] In addition, the peak around 600 nm was due to only $T_1$-$T_n$ transition. The negative bands at 730 nm and 790 nm might be a sum over the positive GSB and the negative photoinduced absorption (PIA), suggesting that the PIA part possesses a larger cross section. Fully understandings of these negative bands require a correct global and target fitting. Despite our efforts in the global fittings, it is suggested that species assisted spectra do not make physical sense of our results. As such, we shall focus only on the negative peaks from 500 nm to 620 nm.

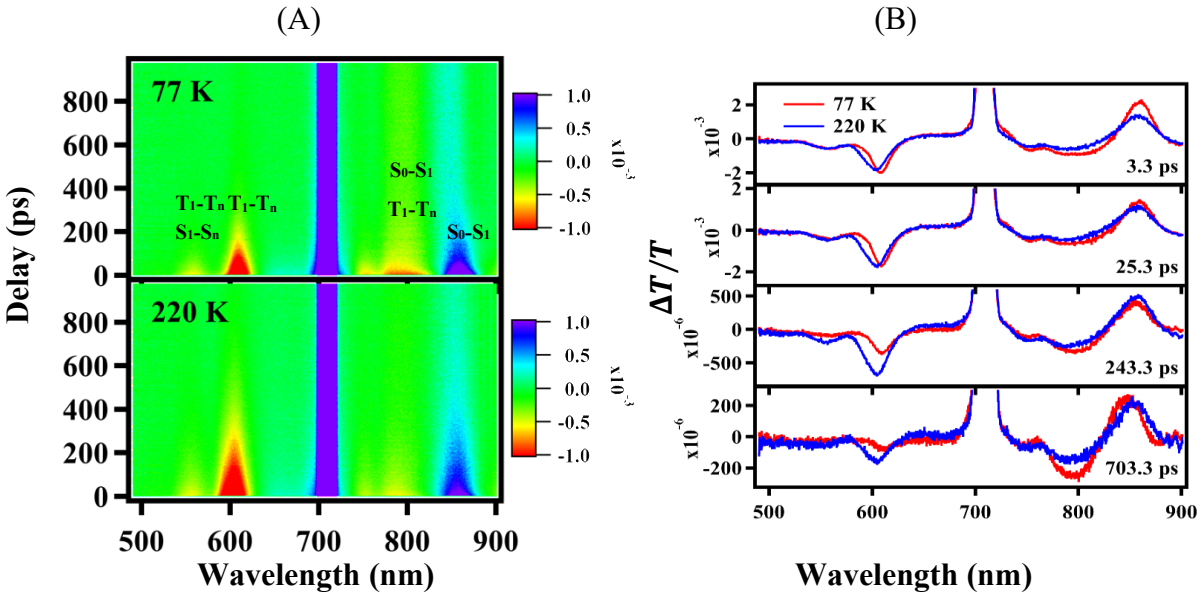


**Figure 2.** (A) Two-dimensional pseudo-color images of transient absorption spectra for polycrystalline hexacene thin films with a pump fluence of 2 μJ/cm$^2$ at 710 nm, under two different temperatures of 77 and 220 K. Shown in (B) are transient spectra ( $\Delta T/T$) under the two different temperatures at the time delays of 3.3, 25.3, 243.3, and 703.3 ps.

Figure 2(B) compares temperature-dependent transient spectra at four different time delays under the two temperatures. As temperature decreases, the transient spectra were red shifted in both the positive GSB and the negative PIA. The spectral red shift in the GS at 860 nm results mainly from a weaker intermolecular coupling when the intermolecular distance of hexacene molecules increases upon thermal expansion. On the other hand, the spectral red-shift of ca. 20 meV was observed in the PIA at 600 nm from room temperature to 77 K. This is possibly due to the fact that a $^1$(T···T) dimer has more available spin microstates antiferromagnetic than its parental $^1$(TT) pair. The relative energetic stability of the $^1$(T···T) is determined by a direct competition between enthalpy and entropy, i.e., $k_B$Tln9. It turns out that the entropy has more contributions than enthalpy for hexacene at the higher temperature, making $^1$(T···T) more stable at room temperature than at 77 K.

We first revealed the effects of temperature on the early dynamics of hexacene. Figure 3 shows temperature-dependent kinetic profiles integrated at 605 nm (A) and 520 nm (B) from the transient spectra of hexacene thin films at a short time scale of 8 ps at five different temperatures, including 77, 100, 140, 180, and 220 K. The upper rows in (A) and (B) are the normalized kinetic traces at 77 K and 220 K for comparison, respectively. At the short time window, the kinetics under all the temperature are similar, as the normalized dynamical behaviors at 77 and 220 K show in the insets of (A) and (B). The early dynamics of hexacene upon photoexcitation is dominated by the formation and dissociation of the correlated biexciton $^1$(TT) at both 605 nm and 520 nm. Thus, global fitting for all the curves were implemented as we did previously.[29] Fittings of kinetics for both the $S_1$ and $^1$(TT) yield the time constants for the formation of $^1$(TT) and the dissociation into $^1$(T···T), being ca, 0.2 and 0.4 ps, respectively, which is consistent with that reported in our early work. [29] The time constants for the two processes under the five temperatures are shown in Table S1. The change in temperature does not affect the singlet fission, including both the formation rate of $^1$(TT) and the dissociation rate into $^1$(T···T).

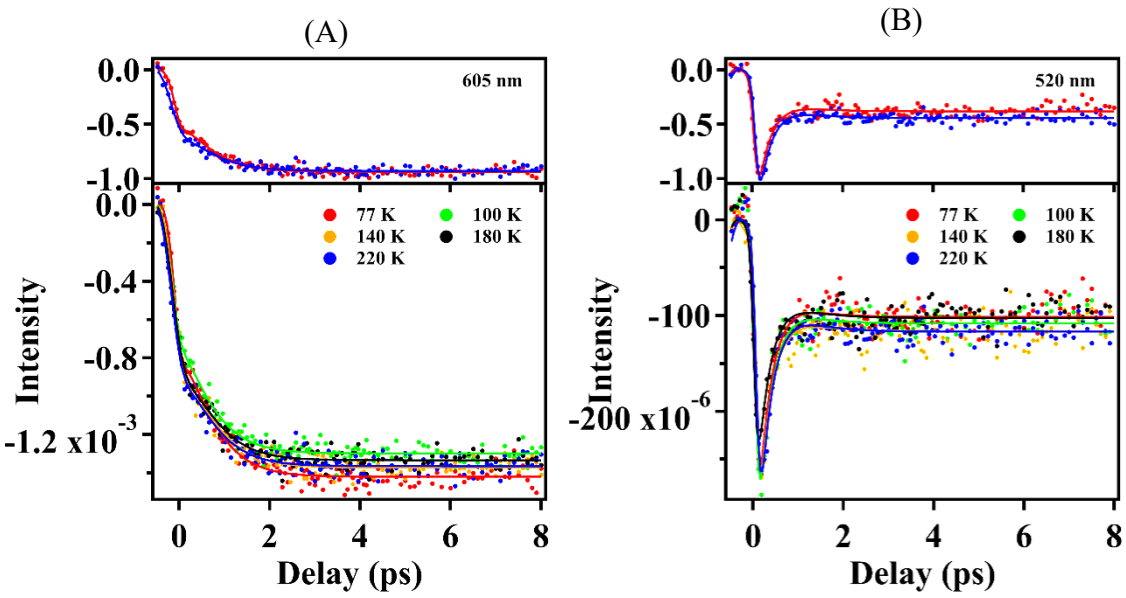


**Figure 3**. Kinetic profiles integrated from 600 - 610 nm (A) and 515-525 nm (B) from the transient spectra of hexacene thin films at 77, 100, 140, 180, and 220 K at a short time scale of 8 ps. The upper rows in (A) and (B) are the normalized kinetic traces at 77 and 220 K for comparison, respectively.

Figure 4 (A) shows kinetic profiles at 605 nm for the transient spectra of hexacene thin films at 77, 100, 140, 180, and 220 K at a long timescale of 950 ps. The dynamical behaviors exhibit more than one exponential recovery for all the temperatures. Intriguingly, the recovery process gets slower in the early stage as temperature increases. A closer comparison of the dynamic curve under 77 and 220 K are shown in the upper row of Figure 4(A). The singlet fission process of photoexcited hexacene is complete. After a few picoseconds, both the singlet exciton and the $^1$(TT) biexciton are converted to $^1$(T···T). Thus, the kinetics for the long-time scale is mainly from the relaxation of $^1$(T···T). We tentatively fitted a double exponential function to the curves for each temperature in Figure 4(A). The faster and slower time constants are on the order of ca. 50 and 200 ps, respectively. These two time constants at different temperatures are plotted in Figure 4(B). Temperature-dependent amplitudes for the two processes from the double exponential fitting are seen in Figure S2. It is seen that the faster recovery process is temperature-independent, while the slower one temperature-dependent. These results suggest that the triplet biexciton recombination of $^1$(T···T) in hexacene experiences different relaxation pathways.

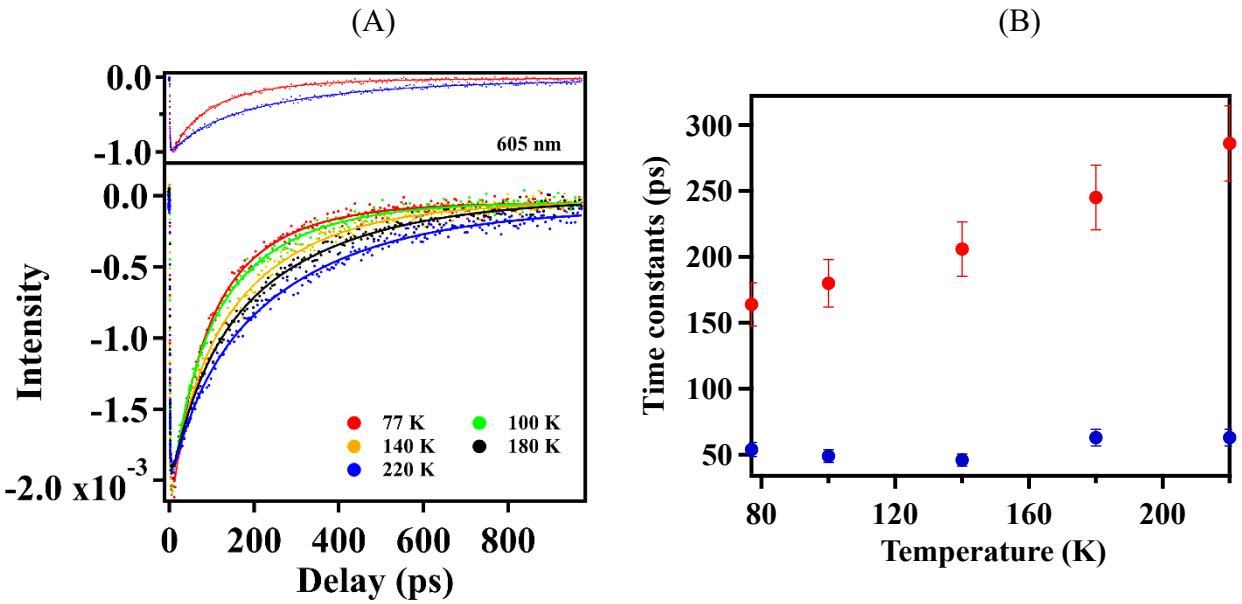


**Figure 4**. (A) Kinetic profiles at 605 nm in the transient spectra for triplet excitons of hexacene thin films at 77, 100, 140, 180, and 220 K at a long-time scale of 950 ps. The upper row in (A) is the normalized kinetic traces at 77 K and 220 K for comparison, respectively. (B) Two time constants extracted from fittings of a double exponential function to the curves in (A) for each temperature.

- **Discussion**

Dynamical processes are significantly affected by high fluence of a pump for hexacene. Fluence-dependent experiments were carried out in our previous work to investigate exciton-exciton

annihilation.[30] The fluence-dependent dynamics of triplet excitons in hexacene indicated that the triplet exciton relaxations from singlet fission proceed in both geminate and non-geminate recombination. Thus, a low fluence of 1.5 μJ/cm$^2$ was used to avoid the exciton-exciton annihilation, in an effort to focus on temperature-dependent singlet fission and triplet excitons in hexacene. Our findings of temperature-dependent singlet fission in hexacene are two-fold: 1) The formation and dissociation processes of $^1$(TT) are independent of temperature. In other words, the singlet fission process does not require thermal activation (non-Arrhenius). Both the formation and dissociation rates of $^1$(TT) are so large that the processes become adiabatic. Such a unique feature is likely due to the large driving force with the big gap between the $S_1$ exciton and $^1$(TT) in hexacene; 2) The $^1$(T···T) state exhibits non-classical temperature-dependent relaxations with more than one exponential function. The triplet excitons in $^1$(T···T) could either recombine in both geminate and non-geminate manners or diffuse away with the loss of spin. The latter generally occurs at more than tens or more nanoseconds and goes beyond our scope here. Our temperature-dependent experiments show that one of the recombination reactions decreases with increasing temperature (anti-Arrhenius). Our temperature-dependent results of hexacene are significantly different from those of tetracene and pentacene reported in the literature.[8-11] These findings suggest that relaxation of triplet excitons of the $^1$(T···T) in hexacene exhibit unique relaxations.

Let us start with triplet excitons in the spatially separated state $^1$(T···T) for hexacene. The triplet excitons in the $^1$(T···T) could interact with either singlet excitons or triplet excitons. It is noted that the triplet-triplet interactions require spin reservations since the singlet spin for $^1$(T···T) is still conserved.[4] In our early work, we have discussed the possibilities of singlet-triplet exciton interactions and triplet–triplet interactions to a higher singlet exciton in the hexacene singlet fission.[30] The singlet excitons, $S_1$, disappear since they last for only 300 fs. As a result, the singlet excitons do not meet triplet excitons at all. On the other hand, triplet–triplet interactions to a higher singlet exciton may not happen due to the fact that the energy gap for the $2T_1$ in hexacene is far below that for the higher singlet exciton level.[29] Thus, we exclude the possibility of the participating singlet excitons in the relaxation of the $^1$(T···T). In the meanwhile, it is possible for the two individual triplet excitons to recombine before the triplet excitons lose spin correlations. When two triplet excitons in the $^1$(T···T) collide each other, the interactions lead to multiple forms. The triplet–triplet interactions inside the $^1$(T···T) could go back to the correlated $^1$(TT) triplet pair or lead to a higher triplet state. The former is so-called geminate recombination of triplet excitons, while the latter non-geminate recombination of triplet excitons. As a matter of fact, the geminate recombination is a reverse process of the dissociation for the $^1$(TT) triplet pair from $^1$(T···T). Ideally, it is anticipated that the $^1$(T···T) is completely converted into two individual $T_1$ for solar energy exploitation. Unlike the ideal case in Eq. 1, the $^1$(T···T) undergoes an additional relaxation channel to $T_n + S_0$ in photoexcited hexacene, resulting in the loss of triplet excitons. As the two triplet excitons in the $^1$(T···T) are approaching, their energy exchange could populate to a triplet energy level of $T_n$ and $S_0$ in hexacene. Thus, a modified kinetic scheme is given by,

$$\mathbf{S_0 + S_1 \longrightarrow {}^1(TT) \leftrightarrows {}^1(T\cdots T) \overset{k_{NG}}{\rightleftarrows} T_n + S_0} \qquad \text{Eq. 2}$$

The population kinetics for the $S_1$, $^1$(TT), and $^1$(T···T) are expressed in three differential equations as,[29]

$$-\frac{dN_{!\,!}}{dt} = k_{"}N_{!\,!}$$

$$\frac{dN_{\#}}{dt} = k_{"}N_{!!} - k_{\$}N_{\#\#} + k_{\%\$}N_{\#\ldots\#}$$
$$\frac{d[T_1]}{dt} = k_{\$}N_{\#\#} - k_{\%\$}N_{\#\ldots\#} - k_{(*}N_{\#\ldots\#} \qquad \text{Eq. 3}$$

where $k_f$ is the rate constants for the formation rate of a correlated triplet pair state, $k_Q$ and $k$-$_Q$ the dissociation rate and its reverse process of a correlated triplet pair state (geminate recombination), and $k_{NG}$ the rate from the $^1$(T···T) to $T_n$ + $S_0$ (non-geminate recombination). Since the lifetimes for the $S_1$ and $^1$(TT) are short, we could only consider the population of the $^1$(T···T) for a long timescale of more than 10 ps as follows,

$$\frac{d[\#\ldots\#]}{dt} = -k_{\%\$}N_{\#\ldots\#} - k_{(*}N_{\#\ldots\#} \qquad \text{Eq. 4}$$

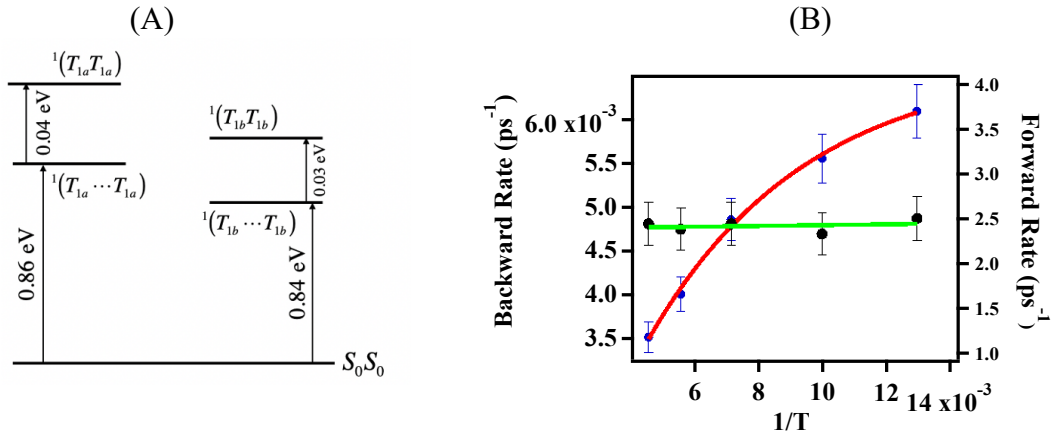


**Figure 5.** (A) Calculated energy diagram for hexacene. (B) Forward ($k_Q$) and backward ($k$-$_Q$) rates from the $^1$(TT) to $^1$(T···T) as a function of temperature, from the fittings in Figures 3 and 4.

The question arises now from how the geminate and nongeminate triplet exciton recombination in hexacene respond to the change in temperature. There are two possible scenarios. The first possibility is that the temperature-dependent and temperature-independent processes are geminate and nongeminate triplet exciton recombination, respectively. The second possibility is the opposite to the first one. To find out the driving force for the recombination, we calculated the energy levels for $^1$(TT) to $^1$(T···T) in hexacene. According to our previously developed functional mode singlet fission theory (FMSF),[44-46] the molecular orbitals of a correlated triplet pair $^1$(TT) can be constructed by the constrained density functional theory (CDFT)[47] through a spatially dependent and spin-polarized Hartree potential that affords a difference of +4 (or -4) on accumulated spins between the two chosen hexacene molecules as reported previously.[29] Similarly, for a spatially separated but spin correlated triplet pair $^1$(T···T), its energy converges to that of an uncorrelated one, $T_1$+$T_1$, due to diminished pair-wise coupling. As a result, our calculated $E_{1(T1T1)}$ is ~0.03 eV higher than $E_{1(T1\ldots T1)}$, which in turn is ~0.85 eV higher than that of the ground state, $E_{S_0S_0}$ as shown in Fig.5(A). If the Marcus non-adiabatic transition theory[48] is employed, the effective activation energy barrier, $\Delta G^{+} = \frac{(-./*\$)^{\%}}{1-}$, for the $^1$(T···T) to $^1$(TT) transition turns out to be rather large at

0.14 eV, where the calculated reorganization energy, $\lambda$, and the driving force, $\Delta G_0$, are 0.64 eV and -0.03 eV, respectively. Therefore, the recombination of triplet excitons in $^1$(T···T) back to $^1$(TT) was assigned to be the temperature-dependent process, while the $^1$(T···T) to ($T_n$ + $S_0$) the temperature-independent.

According to the balance condition,[1, 12-15, 49-50] the ratio of the generation rate to the recombination rate of $^1$(T···T) is written by,

$$\frac{k_{-Q}}{k_Q}(T) \propto e^{-\frac{\Delta E_3}{k_B T}} \quad \text{Eq. 5}$$

where $\Delta E_3$ is the energy difference between the $^1$(T···T) and $^1$(TT), $k_B$ is the Boltzmann constant, and T is the temperature. Figure 5 (B) shows that forward ($k_Q$) and backward ($k_{-Q}$) rates from the $^1$(TT) to $^1$(T···T) as a function of temperature. The best fits of the ratio in the inset yield $\Delta E_a$= E($^1$(TT)) - E($^1$(T···T)) =17.2 meV. Our computational results are consistent with our transient absorption experiments. These results indicate that the spatially separated $^1$(T···T) state relaxes through both the thermally activated and thermally-inactivated processes.

- **Conclusions**

We have utilized temperature-dependent transient absorption spectroscopy to reveal the nature of singlet fission and its subsequent processes in photoexcited hexacene. Our initial goal of this paper was to examine whether the $^1$(TT) intermediate in hexacene might be observed at low temperatures. Unlike those in tetracene and pentacene, no $^1$(TT) intermediate was observed in hexacene. Instead, we found that the formation and dissociation processes of $^1$(TT) in hexacene is independent of temperature. The singlet fission in hexacene does not require thermal activation. Furthermore, it was found that the spatially separated $^1$(T···T) state relaxes through both the thermally-activated and thermally-inactivated processes in hexacene. The temperature-dependent and temperature-independent relaxations of triplet excitons were found to be geminate recombination of $^1$(T···T) and non-geminate triplet-triplet energy transfer, respectively. Our DFT computations supported that the process from the $^1$(TT) to the $^1$(T···T) is favorable in hexacene. Our experimental findings provide new insight into future design of singlet fission materials for desirable triplet exciton exploitations.

## ASSOCIATED CONTENT

### Supporting Information

The cross-correlation of the pump and probe pulses**;** Transient spectra of hexacene at 100, 140, and 180 K; Fitting results of the early dynamics at 520 and 605 nm**;** Global analysis attempts of the dynamics of triplet excitons**;** Discussion of the fitting model for the dynamics at 605 nm.

## AUTHOR INFORMATION

Corresponding Authors: Yi Rao: yi.rao@usu.edu (ORCID:0000-0001-9882-1314), and Hanning Chen: hchen@american.edu (ORCID: 0000-0003-3568-8039).

## ACKNOWLEDGMENTS

The authors are grateful for funding support from Honda Research Institute, San Jose, USA. Y.R. was supported by the National Science Foundation under Grant No. 2045084. Computational resources were provided by the Argonne Leadership Computing Facilities at Argonne National Laboratory under Department of Energy contract DE-AC-06CH11357 and by the Extreme Science and Engineering Discovery Environment at Texas Advanced Computing Center under National Science Foundation contract TG-CHE130008.

**References**

(1) Smith, M. B.; Michl, J., Singlet Fission. *Chem. Rev.* **2010**, *110*, 6891-6936.
(2) Smith, M. B.; Michl, J., Recent Advances in Singlet Fission. *Annu. Rev. Phys. Chem.* **2013**, *64*, 361-386.
(3) Merrifield, R. E.; Avakian, P.; Groff, R. P., Fission of Singlet Excitons into Pairs of Triplet Excitons in Tetracene Crystals. *Chemical Physics Letters* **1969**, *3*, 155-157.
(4) Scholes, G. D., Correlated Pair States Formed by Singlet Fission and Exciton–Exciton Annihilation. *J. Phys. Chem. A* **2015**, *119*, 12699-12705.
(5) Frankevich, E. L.; Lesin, V. I.; Pristupa, A. I., Rate Constants of Singlet Exciton Fission in a Tetracene Crystal Determined from the Rydmr Spectral Linewidth. *Chem. Phys. Lett.* **1978**, *58*, 127-131.
(6) Burdett, J. J.; Bardeen, C. J., Quantum Beats in Crystalline Tetracene Delayed Fluorescence Due to Triplet Pair Coherences Produced by Direct Singlet Fission. *J. Am. Chem. Soc.* **2012**, *134*, 8597-8607.
(7) Pensack, R. D.; Ostroumov, E. E.; Tilley, A. J.; Mazza, S.; Grieco, C.; Thorley, K. J.; Asbury, J. B.; Seferos, D. S.; Anthony, J. E.; Scholes, G. D., Observation of Two Triplet-Pair Intermediates in Singlet Exciton Fission. *The Journal of Physical Chemistry Letters* **2016**, *7*, 2370-2375.
(8) Stern, H. L., et al., Vibronically Coherent Ultrafast Triplet-Pair Formation and Subsequent Thermally Activated Dissociation Control Efficient Endothermic Singlet Fission. *Nature Chem.* **2017**, *9*, 1205-1212.
(9) Wilson, M. W. B.; Rao, A.; Johnson, K.; Gélinas, S.; di Pietro, R.; Clark, J.; Friend, R. H., Temperature-Independent Singlet Exciton Fission in Tetracene. *J. Am. Chem. Soc.* **2013**, *135*, 16680-16688.
(10) Wan, Y.; Wiederrecht, G. P.; Schaller, R. D.; Johnson, J. C.; Huang, L., Transport of Spin-Entangled Triplet Excitons Generated by Singlet Fission. *J. Phys. Chem. Lett.* **2018**, *9*, 6731-6738.
(11) Lee, T. S.; Lin, Y. L.; Kim, H.; Rand, B. P.; Scholes, G. D., Two Temperature Regimes of Triplet Transfer in the Dissociation of the Correlated Triplet Pair after Singlet Fission. *Can. J. Chem.* **2019**, *97*, 465-473.
(12) Li, J.; Chen, Z.; Zhang, Q.; Xiong, Z.; Zhang, Y., Temperature-Dependent Singlet Exciton Fission Observed in Amorphous Rubrene Films. *Org. Electron.* **2015**, *26*, 213-217.
(13) Ma, L.; Zhang, K.; Kloc, C.; Sun, H.; Michel-Beyerle, M. E.; Gurzadyan, G. G., Singlet Fission in Rubrene Single Crystal: Direct Observation by Femtosecond Pump–Probe Spectroscopy. *Phys. Chem. Chem. Phys.* **2012**, *14*, 8307-8312.
(14) Müller, A. M.; Avlasevich, Y. S.; Schoeller, W. W.; Müllen, K.; Bardeen, C. J., Exciton Fission and Fusion in Bis(Tetracene) Molecules with Different Covalent Linker Structures. *J. Am. Chem. Soc.* **2007**, *129*, 14240-14250.

(15) Ma, L.; Zhang, K.; Kloc, C.; Sun, H.; Soci, C.; Michel-Beyerle, M. E.; Gurzadyan, G. G., Fluorescence from Rubrene Single Crystals: Interplay of Singlet Fission and Energy Trapping. *Phys. Rev. B* **2013**, *87*, 201203.
(16) Lee, T. S.; Lin, Y. L.; Kim, H.; Pensack, R. D.; Rand, B. P.; Scholes, G. D., Triplet Energy Transfer Governs the Dissociation of the Correlated Triplet Pair in Exothermic Singlet Fission. *J. Phys. Chem. Lett.* **2018**, *9*, 4087-4095.
(17) Piland, G. B.; Bardeen, C. J., How Morphology Affects Singlet Fission in Crystalline Tetracene. *The Journal of Physical Chemistry Letters* **2015**, *6*, 1841-1846.
(18) Burdett, J. J.; Gosztola, D.; Bardeen, C. J., The Dependence of Singlet Exciton Relaxation on Excitation Density and Temperature in Polycrystalline Tetracene Thin Films: Kinetic Evidence for a Dark Intermediate State and Implications for Singlet Fission. *J. Chem. Phys.* **2011**, *135*, 214508.
(19) Tayebjee, M. J. Y.; Clady, R. l. G. C. R.; Schmidt, T. W., The Exciton Dynamics in Tetracene Thin Films. *Phys. Chem. Chem. Phys.* **2013**, *15*, 14797-14805.
(20) Poletayev, A. D.; Clark, J.; Wilson, M. W. B.; Rao, A.; Makino, Y.; Hotta, S.; Friend, R. H., Triplet Dynamics in Pentacene Crystals: Applications to Fission-Sensitized Photovoltaics. *Adv. Mater.* **2014**, *26*, 919-924.
(21) Bayliss, S. L.; Chepelianskii, A. D.; Sepe, A.; Walker, B. J.; Ehrler, B.; Bruzek, M. J.; Anthony, J. E.; Greenham, N. C., Geminate and Nongeminate Recombination of Triplet Excitons Formed by Singlet Fission. *Physical Review Letters* **2014**, *112*, 238701.
(22) Thompson, N. J.; Hontz, E.; Congreve, D. N.; Bahlke, M. E.; Reineke, S.; Van Voorhis, T.; Baldo, M. A., Nanostructured Singlet Fission Photovoltaics Subject to Triplet-Charge Annihilation. *Adv. Mater.* **2014**, *26*, 1366-1371.
(23) Seki, K.; Sonoda, Y.; Katoh, R., Diffusion-Mediated Delayed Fluorescence by Singlet Fission and Geminate Fusion of Correlated Triplets. *J. Phys. Chem. C* **2018**, *122*, 11659-11670.
(24) Wan, Y.; Guo, Z.; Zhu, T.; Yan, S.; Johnson, J.; Huang, L., Cooperative Singlet and Triplet Exciton Transport in Tetracene Crystals Visualized by Ultrafast Microscopy. *Nature Chem.* **2015**, *7*, 785-792.
(25) Grieco, C.; Doucette, G. S.; Pensack, R. D.; Payne, M. M.; Rimshaw, A.; Scholes, G. D.; Anthony, J. E.; Asbury, J. B., Dynamic Exchange During Triplet Transport in Nanocrystalline Tips-Pentacene Films. *J. Am. Chem. Soc.* **2016**, *138*, 16069-16080.
(26) Cruz, C. D.; Choi, H. H.; Podzorov, V.; Chronister, E. L.; Bardeen, C. J., Photon Upconversion in Crystalline Rubrene: Resonant Enhancement by an Interband State. *J. Phys. Chem. C* **2018**, *122*, 17632-17642.
(27) Pensack, R. D., et al., Solution-Processable, Crystalline Material for Quantitative Singlet Fission. *Materials Horizons* **2017**, *4*, 915-923.
(28) Hudson, R. J.; Huang, D. M.; Kee, T. W., Anisotropic Triplet Exciton Diffusion in Crystalline Functionalized Pentacene. *J. Phys. Chem. C* **2020**, *124*, 23541-23550.
(29) Sun, D., et al., Anisotropic Singlet Fission in Single Crystalline Hexacene. *iScience* **2019**, *19*, 1079-1089.
(30) Han, J.; Xie, Q.; Luo, J.; Deng, G.-H.; Qian, Y.; Sun, D.; Harutyunyan, A. R.; Chen, G.; Rao, Y., Anisotropic Geminate and Non-Geminate Recombination of Triplet Excitons in Singlet Fission of Single Crystalline Hexacene. *The Journal of Physical Chemistry Letters* **2020**, *11*, 1261-1267.
(31) Piland, G.; Grumstrup, E. M., High-Repetition Rate Broadband Pump–Probe Microscopy. *J. Phys. Chem. A* **2019**, *123*, 8709-8716.

(32) Grumstrup, E. M., Spatiotemporal Coupling of Excited State Dynamics in Time-Resolved Microscopies. *Opt. Express* **2019**, *27*, 31385-31393.
(33) Watanabe, M.; Chang, Y. J.; Liu, S.-W.; Chao, T.-H.; Goto, K.; Islam, M. M.; Yuan, C.-H.; Tao, Y.-T.; Shinmyozu, T.; Chow, T. J., The Synthesis, Crystal Structure and Charge-Transport Properties of Hexacene. *Nature Chem.* **2012**, *4*, 574-578.
(34) Deng, G.-H.; Wei, Q.; Han, J.; Qian, Y.; Luo, J.; Harutyunyan, A. R.; Chen, G.; Bian, H.; Chen, H.; Rao, Y., Vibronic Fingerprint of Singlet Fission in Hexacene. *J. Chem. Phys.* **2019**, *151*, 054703.
(35) Warshel, A.; Levitt, M., Theoretical Studies of Enzymic Reactions: Dielectric, Electrostatic and Steric Stabilization of the Carbonium Ion in the Reaction of Lysozyme. *J. Mol. Biol.* **1976**, *103*, 227-249.
(36) Hohenberg, P.; Kohn, W., Inhomogeneous Electron Gas. *Phys. Rev.* **1964**, *136*, B864-B871.
(37) Wang, J.; Wolf, R. M.; Caldwell, J. W.; Kollman, P. A.; Case, D. A., Development and Testing of a General Amber Force Field. *J. Comput. Chem.* **2004**, *25*, 1157-1174.
(38) Kühne, T. D., et al., Cp2k: An Electronic Structure and Molecular Dynamics Software Package - Quickstep: Efficient and Accurate Electronic Structure Calculations. *J. Chem. Phys.* **2020**, *152*, 194103.
(39) Goedecker, S.; Teter, M.; Hutter, J., Separable Dual-Space Gaussian Pseudopotentials. *Phys. Rev. B* **1996**, *54*, 1703-1710.
(40) Woon, D. E.; Dunning, T. H., Gaussian Basis Sets for Use in Correlated Molecular Calculations. Iv. Calculation of Static Electrical Response Properties. *J. Chem. Phys.* **1994**, *100*, 2975-2988.
(41) Sun, H.; Zhong, C.; Brédas, J.-L., Reliable Prediction with Tuned Range-Separated Functionals of the Singlet–Triplet Gap in Organic Emitters for Thermally Activated Delayed Fluorescence. *J. Chem. Theory Comput.* **2015**, *11*, 3851-3858.
(42) Laino, T.; Mohamed, F.; Laio, A.; Parrinello, M., An Efficient Real Space Multigrid Qm/Mm Electrostatic Coupling. *J. Chem. Theory Comput.* **2005**, *1*, 1176-1184.
(43) Genovese, L.; Deutsch, T.; Neelov, A.; Goedecker, S.; Beylkin, G., Efficient Solution of Poisson's Equation with Free Boundary Conditions. *J. Chem. Phys.* **2006**, *125*, 074105.
(44) Elenewski, J. E.; Cubeta, U. S.; Ko, E.; Chen, H., Functional Mode Singlet Fission Theory. *J. Phys. Chem. C* **2017**, *121*, 4130-4138.
(45) Elenewski, J. E.; Cubeta, U. S.; Ko, E.; Chen, H., Computer Simulation of Singlet Fission in Single Crystalline Pentacene by Functional Mode Vibronic Theory. *J. Phys. Chem. C* **2017**, *121*, 11159-11165.
(46) Deng, G.-H.; Qian, Y.; Li, X.; Zhang, T.; Jiang, W.; Harutyunyan, A. R.; Chen, G.; Chen, H.; Rao, Y., Singlet Fission Driven by Anisotropic Vibronic Coupling in Single-Crystalline Pentacene. *J. Phys. Chem. Lett.* **2021**, *12*, 3142-3150.
(47) Wu, Q.; Van Voorhis, T., Direct Optimization Method to Study Constrained Systems within Density-Functional Theory. *Phys. Rev. A* **2005**, *72*, 024502.
(48) Marcus, R. A., Chemical and Electrochemical Electron-Transfer Theory. *Annu. Rev. Phys. Chem.* **1964**, *15*, 155-196.
(49) Groff, R. P.; Avakian, P.; Merrifield, R. E., Coexistence of Exciton Fission and Fusion in Tetracene Crystals. *Phys. Rev. B* **1970**, *1*, 815-817.
(50) Berkelbach, T. C.; Hybertsen, M. S.; Reichman, D. R., Microscopic Theory of Singlet Exciton Fission. Ii. Application to Pentacene Dimers and the Role of Superexchange. *J. Chem. Phys.* **2013**, *138*, 114103.

TOC Graphic

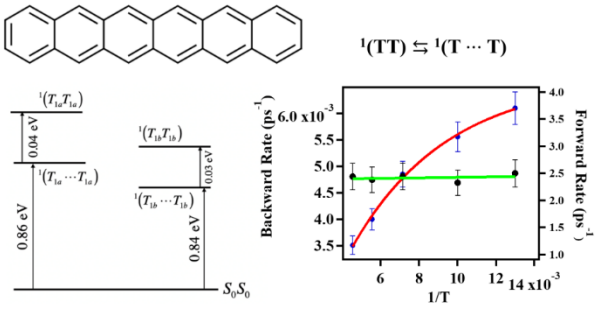
$^1(TT) \leftrightarrows {}^1(T \cdots T)$
$^1(T_{1a}T_{1a})$
0.04 eV
$^1(T_{1a}\cdots T_{1a})$
0.86 eV
$S_0S_0$
$^1(T_{1b}T_{1b})$
0.03 eV
$^1(T_{1b}\cdots T_{1b})$
0.84 eV
Backward Rate (ps$^{-1}$)
Forward Rate (ps$^{-1}$)
6.0 x10$^{-3}$
5.5
5.0
4.5
4.0
3.5
4.0
3.5
3.0
2.5
2.0
1.5
1.0
6
8
10
12
14 x10$^{-3}$
1/T